Delft University of Technology

Influence of Measurement Uncertainty on Parameter Estimation and Fault Location for Transmission Lines

Fu, Jianfeng; Song, Guobing; De Schutter, Bart

Important note
To cite this publication, please use the final published version (if applicable).
Please check the document version above.

Influence of Measurement Uncertainty on Parameter Estimation and Fault Location for Transmission Lines

Jianfeng Fu , Guobing Song , *Member, IEEE*, and Bart De Schutter , *Fellow, IEEE*

(Invited Paper)

Abstract—Fault location algorithms for transmission lines use the parameters of the transmission line to locate faults after the faults have occurred along the line. Although these parameters can be estimated by the phasor measurement units (PMUs) at the terminal(s) of the transmission line continuously, the uncertainty in the measurements will give rise to stochastic errors in the measured values. Thus, the uncertainty in measurements definitely influences the estimations of the parameters of the transmission line, which, in turn, influences the results of fault location algorithms. Inaccurate results of fault location algorithms may lead to costly maintenance fees and prolonged outage time. Therefore, in this article, we estimate the parameters of the transmission line considering the uncertainty in the measurements so that a more accurate fault location can be derived. The uncertainty in the measurements will be modeled as a stochastic distribution, and the maximum likelihood estimation (MLE) method will be adopted to reduce the uncertainty in the measurements. In addition, as an illustration, the telegrapher's equations will be used to calculate the parameters of the transmission line, and the two-terminal positive sequence network fault location algorithm will be used to locate the fault. In a simulation, a case study of a real-life transmission line the influence of the uncertainty in the measurements on the transmission line parameter estimations and the effectiveness of the MLE method for estimations are simulated and analyzed. The results show that the influence of the uncertainty in the measurements on the positive sequence network fault location algorithm should not be neglected and that the proposed method is very effective in significantly reducing the influence of the uncertainty in the measurements.

Note to Practitioners—The objective of this article is to address the significant effects of inaccuracies in the measurements for fault location determination in transmission lines in power systems. These inaccuracies increase the cost and duration of the search process for the actual fault location, and they, thus, also enlarge the outage duration and reduce the power system reliability. This article aims to analyze and reduce the influence of the uncertainties in the measurements in order to obtain a much more accurate fault location estimate when a fault has occurred along the transmission line. One of the key contributions of this article is the development of a model for the uncertainties in the measurements based on a confidence level and deviation bounds; this model can then be used if the information on the distributions of the uncertainties in the measurements is not available. Another key contribution is a maximum likelihood estimation method to estimate line parameters more accurately and consequently to reduce the influence of the uncertainties in the measurements on the fault location estimate.

Index Terms—Fault location, maximum likelihood estimation (MLE), transmission line parameter estimation, uncertainty in measurements.

I. INTRODUCTION

FAULT location algorithms for transmission lines are used to locate the fault after a fault along the transmission line has occurred and they are operated by protection relay devices [1]–[4]. After that, the maintenance team of the transmission line operator searches the area near the located spot that is calculated by fault location algorithms to find out where exactly the fault is and then performs maintenance actions to resolve the fault. For a given transmission line, a large deviation between the exact fault location and the evaluated fault location may emerge when the evaluated location is derived from an inaccurate fault location algorithm. This deviation will enlarge the search burden, searching costs, and the unavailability period of the faulty transmission line. For example, for a 300-km-long transmission line lying beneath the continental shelf in a sea area, a 1% deviation in the location will give rise to a ± 3-km gap between the exact fault location, and the evaluated fault location and searching such a large area in the sea is extremely costly. Thus, the accuracy of the fault location algorithm is very relevant for the reduction of the costs in power system maintenance [5], [6].

At present, in the literature on fault location algorithms, factors related to the inaccuracy of the fault location algorithms are discussed and analyzed as follows.

First, the generation of the dc offset and harmonics during the fault transient stage by the faults results in the inaccuracy of the voltage and current phasor calculations and, thus, inaccuracy of the fault location algorithms [7]–[12]. These factors are usually considered as additional signals added to the fundamental signals. Thus, the solution approach to address this factor is mainly related to signal transformations (or filters). For example, the article [7] proposes a new

application of Park's transformation to calculate fundamental components among the sampled voltages and currents that are distorted by the dc offset and harmonics. Tajdinian *et al.* [8] proposed a method for the phasor calculation of the fundamental component by obtaining the dc amplitude from the Hilbert transform and the fault current signals within 20 ms. The article [9] proposes a method for removing the exponential component among the electrical signals in the transient stage to evaluate the fundamental frequency phasor.

Second, noise and disturbances caused by the external environment also result in the inaccuracy of fault location algorithms [13], [14]. This factor is usually addressed by robust filters or transformations. For example, the article [13] proposed an approach for the protection of parallel transmission lines by using the S-transform that is an extension of the wavelet transform. The test results show the robustness of the proposed algorithm by adding significant noise to the simulated voltage and current. In [14], a pattern recognition approach with a new S-transform method is proposed by using different types of techniques, e.g., frequency scaling, to reduce the computational cost and to remove redundant information. The simulation results show the robustness of the proposed algorithm in an environment with significant noise.

It can be concluded that the influences of the dc offset and harmonics during the transient stages on the fault location algorithms can be reduced in a systematic way by using a patched algorithm and that the influence of some noises and disturbances can be reduced by designing a more robust algorithm. Apart from these factors, the fault location algorithms are also influenced by inaccuracies regarding the values of the transmission line parameters. For example, a transmission line might be put into practice in summer, and the parameters are measured and recorded before its putting into use. Then, under a fault that occurs in winter, the fault location results are no longer accurate when the parameters recorded in summer are used. In addition, the inaccuracies of the parameters may also result from different humidity and temperature circumstances. However, these factors can be addressed by the increasing popularization of phasor measurement units (PMUs) that are installed at the terminal(s) of the transmission line. Installed PMUs can measure the transmission line parameters continuously by using the voltage and current phasors collected and calculated from the instruments and the computing unit inside the PMUs [15]–[17]. However, the uncertainty in PMU measurements emerges during the calculation of the phasors, which will lead to inaccuracies of the calculated transmission line parameters. For example, articles [18]–[21] reveal the uncertainty phenomena and mechanisms during the transmission line measurement by PMUs. In the article [18], the systematic errors in the measurements are assumed to be constant values when calculating the transmission line parameters. However, articles [19]–[22] reveal that the error between the exact value and the measured value cannot be properly evaluated nor corrected because of the multitude of influential factors, e.g., humidity, temperature, and load level on top of the systematic errors; Sivanagaraju *et al.* [19], Asprou *et al.* [20], Milojević *et al.* [21], and Manousakis *et al.* [22] recommend to use the uncertainty to describe the possibility distribu-
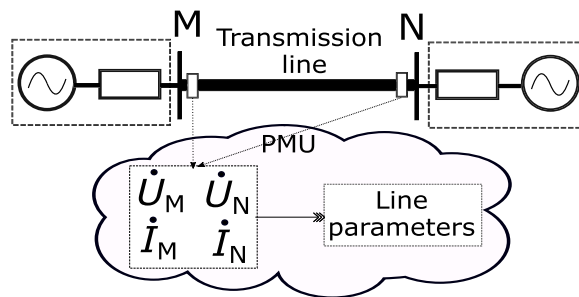

Fig. 1.   Mechanism for estimations of line parameters.

tion of the error in the measurements. In [19] and [20], the bounds of the uncertainties in the measurements are analyzed and calculated for ensuring the reliability of protection relay algorithms. However, these bounds cannot be applied in fault location algorithms because the bounds will lead to conservative results. In addition, Suonan *et al.* [23] and Yuansheng *et al.* [24] have analyzed the influence of all the uncertainties of the transmission line parameters on fault location algorithms, but they do not model the uncertainty in the measurement specifically nor do they propose a method to calculate and reduce the influence due to the uncertainties in the measurements of PMUs on transmission line parameters.

Thus, it can be concluded from the literature that a lot of work still needs to be done on the analysis of the influence of the uncertainty in the measurements on the behavior of fault location algorithms. Furthermore, the uncertainty in the measurements should be addressed properly. Both topics will be addressed in this article. Thus, the contribution of this article can be summarized as follows. First, we analyze the influence of the uncertainty in the measurements on the fault location algorithms based on a case study. Second, we model the uncertainty in the measurements of PMUs based on the information supplied by the PMU supplier or by a newly proposed method based on the confidence level and deviation bounds if the information on the distributions of the uncertainties is not available. Third, we propose an estimation method based on maximum likelihood estimation (MLE) that can effectively reduce the uncertainty in the measurements when determining the transmission line parameters.

This article is organized as follows. In Section II, the modeling method for the uncertainty in the transmission line parameter measurements is introduced. In Section III, a method is proposed to obtain the distributions of the uncertainties based on the data provided by the device supplier or by using big data methods. In Section IV, a method is given to reduce the influence of the uncertainty in the measurements. In Section V, a case study is presented to show and analyze the influence of the uncertainty in the measurements on the two-terminal positive sequence network fault location algorithm as well as the effectiveness of the proposed method. In Section VI, conclusions are drawn, and some topics for future work are discussed.

II. TRANSMISSION LINE PARAMETERS CALCULATION MODEL WITH UNCERTAINTIES

The transmission line parameters measurement process is shown in Fig. 1. In Fig. 1, the voltage and current phasors

from the M and N terminals of the line are marked as $\dot{U}_\text{M}$, $\dot{U}_\text{N}$, $\dot{I}_\text{M}$, and $\dot{I}_\text{N}$. The phasors collected from the PMUs at the two terminals will be used to calculate the transmission line parameters. In the view of the single phase of the transmission line [25], [26], the telegrapher's equation of the voltage and current phasor from both two terminals can be described as

$$\begin{cases} \dot{U}_\text{M} = \dot{U}_\text{N}\cosh(\gamma D) - \dot{I}_\text{N}z_\text{c}\sinh(\gamma D) \\ \dot{I}_\text{M} = \dot{U}_\text{N}\sinh(\gamma D)/z_\text{c} - \dot{I}_\text{N}\cosh(\gamma D) \end{cases} \tag{1}$$

where γ is the propagation constant of the transmission line, z_c is the characteristic impedance of the transmission line, and D is the length of the transmission line. According to (1), γ and z_c can be obtained as

$$\begin{cases} \gamma = \dfrac{1}{D}\cosh^{-1}\dfrac{\dot{U}_\text{M}\dot{I}_\text{M} - \dot{U}_\text{N}\dot{I}_\text{N}}{\dot{U}_\text{N}\dot{I}_\text{M} - \dot{U}_\text{M}\dot{I}_\text{N}} \\ z_\text{c} = \sqrt{(\dot{U}_\text{M}^2 - \dot{U}_\text{N}^2)/(\dot{I}_\text{M}^2 - \dot{I}_\text{N}^2)}. \end{cases} \tag{2}$$

Thus, the transmission line parameters of the positive sequence network can be derived as [27]–[29]

$$\begin{cases} z_1 = \gamma z_\text{c} = r_1 + \mathrm{i}x_1 \\ y_1 = \gamma/z_\text{c} = \mathrm{i}b_1 \end{cases} \tag{3}$$

where z_1 and y_1 are, respectively, the positive sequence impedance and admittance of the unit length; r_1, x_1, and b_1 are the positive sequence resistance, reactance, and conductance; and i represents the unit imaginary number. It should be mentioned that because the value of the susceptance is rather small, the susceptance is neglected mostly in fault location algorithms for transmission lines. Thus, we do not consider the susceptance. Thus, z_1 and y_1 can be obtained based on (2) and (3), such that

$$\begin{cases} z_1 = r_1 + \mathrm{i}x_1 = \gamma z_\text{c} \\ y_1 = \mathrm{i}b_1 = \gamma/z_\text{c} \\ \gamma = \dfrac{1}{D}\cosh^{-1}\left(\dfrac{U_\text{M}I_\text{M}\angle(\theta_\text{M} + \phi_\text{M}) - U_\text{N}I_\text{N}\angle(\theta_\text{N} + \phi_\text{N})}{U_\text{N}I_\text{M}\angle(\theta_\text{N} + \phi_\text{M}) - U_\text{M}I_\text{N}\angle(\theta_\text{M} + \phi_\text{N})}\right) \\ z_\text{c} = \sqrt{\dfrac{(U_\text{M})^2\angle(2\theta_\text{M}) - (U_\text{N})^2\angle(2\theta_\text{N})}{(I_\text{M})^2\angle(2\phi_\text{M}) - (I_\text{N})^2\angle(2\phi_\text{N})}}. \end{cases} \tag{4}$$

However, the error between the exact value and measured value should be considered in order to obtain more accurate parameter estimations. In addition, this error cannot be evaluated properly and corrected because of its complex influential factors, e.g., the humidity, temperature, and load. According to the guide to express the uncertainty in the measurements (GUM) that is published by the joint working group of the International Electrotechnical Commission (IEC), the International Organization for Standardization (ISO), and so on [30], the uncertainty in the measurements can be used to describe the distribution of the error deviations where the error in the measurements is seen as a stochastic variable.

Thus, if we define the voltage or current phasor at the M or N terminal as the combination of the amplitudes and angles, the collected value vectors from the PMUs can be expressed as $X_\text{collect}^\text{amp} = [U_\text{M}^\text{c}\ U_\text{N}^\text{c}\ I_\text{M}^\text{c}\ I_\text{N}^\text{c}]^\text{T}$ and $X_\text{collect}^\text{ang} = [\theta_\text{M}^\text{c}\ \theta_\text{N}^\text{c}\ \phi_\text{M}^\text{c}\ \phi_\text{N}^\text{c}]^\text{T}$, where U^c and θ^c are, respectively, the voltage amplitude and

TABLE I
MAXIMUM UNCERTAINTY IN MEASUREMENTS

Voltage amplitude (%)	Current amplitude (%)	Voltage angle (degree)	Current angle (degree)
1	1	0.667	1

angle of collected voltage phasors at the M and N terminals, and I^c and ϕ^c are the current amplitude and angle of collected current phasors at the M and N terminals. Furthermore, the true value vector of the actual phasors can be expressed as $X_\text{true}^\text{amp} = [U_\text{M}^\text{t}\ U_\text{N}^\text{t}\ I_\text{M}^\text{t}\ I_\text{N}^\text{t}]^\text{T}$ and $X_\text{true}^\text{ang} = [\theta_\text{M}^\text{t}\ \theta_\text{N}^\text{t}\ \phi_\text{M}^\text{t}\ \phi_\text{N}^\text{t}]^\text{T}$, where U^t and θ^t are, respectively, the voltage amplitude and angle of true voltage phasors at the M and N terminals, and I^t and ϕ^t are the current amplitude and angle of true current phasors at the M and N terminals. Then, we define two 4-D vectors $e^\text{amp} = [e_\text{MU}\ e_\text{NU}\ e_\text{MI}\ e_\text{NI}]^\text{T}$ as the errors between $X_\text{collect}^\text{amp}$ and X_true^amp and $e^\text{ang} = [e_{\text{M}\theta}\ e_{\text{N}\theta}\ e_{\text{M}\phi}\ e_{\text{N}\phi}]^\text{T}$ as the errors between $X_\text{collect}^\text{ang}$ and X_true^ang, such that

$$\begin{aligned} X_\text{collect}^\text{amp} &= X_\text{true}^\text{amp} \odot (1_{4\times 1} + e^\text{amp}) \\ X_\text{collect}^\text{ang} &= X_\text{true}^\text{ang} + e^\text{ang} \end{aligned} \tag{5}$$

where $1_{4\times 1}$ is the unit vector of four rows, and the symbol $\odot$ represents the Hadamard product.

III. MODEL THE UNCERTAINTIES IN THE MEASUREMENTS

To model the uncertainty in the measurements, the amplitude error e^amp and angle error e^ang are considered as stochastic variables subject to specific distributions. These specific distributions of errors can be given by the supplier of the PMU or by big data algorithms, e.g., [31]. In the worst case that no distributions of errors are available, the maximum bound of the uncertainty in the measurements of the PMU will usually be known [32], [33], and the normal distribution will be recommended to model the distribution of errors as indicated in the GUM. For instance, assuming that no information about the distributions of the errors is available, however, the maximum uncertainty in the measurements of one certain PMU using the 1S accuracy class current and voltage transformers is given, as listed in Table I [33]. Based on the character of the standard deviation in the normal distribution, the maximum uncertainty boundaries can be approximately seen as end points of the confidence interval between $\mu \pm 3\sigma$ (the error has 99.7% possibility to lie in this interval), where μ and σ are the expectation and standard deviation of the normal distribution, and as a result, the distribution of error can be obtained. Define f_e^amp and f_e^ang as the probability density function (pdf) of e^amp and e^ang individually, where $f_e^\text{amp} = [f_{e_\text{MU}}^\text{amp}\ f_{e_\text{NU}}^\text{amp}\ f_{e_\text{MI}}^\text{amp}\ f_{e_\text{NI}}^\text{amp}]^\text{T}$ and $f_e^\text{ang} = [f_{e_\text{MU}}^\text{ang}\ f_{e_\text{NU}}^\text{ang}\ f_{e_\text{MI}}^\text{ang}\ f_{e_\text{NI}}^\text{ang}]^\text{T}$.

IV. REDUCE THE UNCERTAINTY IN MEASUREMENTS

In order to evaluate the true values defined as $\hat{X}_\text{true}^\text{amp}$ and $\hat{X}_\text{true}^\text{ang}$ by using the collected values and pdfs of e^amp and e^ang, theoretically, both the MLE method and the method of moments can be used. However, considering the case that all the errors are subject to the normal distribution, the expectation and variance of $X_\text{collect}^\text{amp}$ are both related to the parameter $\hat{X}_\text{true}^\text{ang}$

that is required to be estimated. Simply using the least squares method (for the first moment) to estimate the parameter $\hat{X}_{\text{true}}^{\text{ang}}$ will lead to a loss of accuracy because of neglecting the variance of $X_{\text{collect}}^{\text{ang}}$. Thus, the MLE method is a better method to address the estimation problem. Therefore, we introduce the MLE method to estimate undetermined parameters as follows.

1) Derive PDFs: According to the pdfs of e^{amp} and e^{ang} as well as (5), the pdfs f_e^{amp} and f_e^{ang} of $X_{\text{collect}}^{\text{amp}}$ and $X_{\text{collect}}^{\text{ang}}$ can be obtained such that

$$f_{x^{\text{amp}}}(X_{\text{collect}}^{\text{amp}}) = f_{x^{\text{amp}}}(X_{\text{true}}^{\text{amp}} \circ (I_{8\times1} + e^{\text{amp}}))$$
$$f_{x^{\text{ang}}}(X_{\text{collect}}^{\text{ang}}) = f_{x^{\text{ang}}}(X_{\text{true}}^{\text{ang}} + e^{\text{ang}}) \tag{6}$$

where $X_{\text{true}}^{\text{amp}}$ and $X_{\text{true}}^{\text{ang}}$ are values required to be evaluated.

2) MLE: According to (6) and using the sampling points $X_{\text{collect}}^{\text{amp}}(t_0 - n)$ to $X_{\text{collect}}^{\text{amp}}(t_0)$ and $X_{\text{collect}}^{\text{ang}}(t_0 - n)$ to $X_{\text{collect}}^{\text{ang}}(t_0)$, the maximum likelihood functions can be expressed as

$$L(\hat{X}_{\text{true}}^{\text{amp}}) = \sup_{X_{\text{true}}^{\text{amp}}} \prod_{k=1}^{n} p(X_{\text{collect}}^{\text{amp}} \mid X_{\text{true}}^{\text{amp}}(k))$$

$$L(\hat{X}_{\text{true}}^{\text{ang}}) = \sup_{X_{\text{true}}^{\text{ang}}} \prod_{k=1}^{n} p(X_{\text{collect}}^{\text{ang}} \mid X_{\text{true}}^{\text{ang}}(k)) \tag{7}$$

where $L(\cdot)$ is the MLE function and $p(X_{\text{collect}}^{\text{amp}} \mid X_{\text{true}}^{\text{amp}}(k))$ is the probability of $X_{\text{collect}}^{\text{amp}}(k)$ that can be expressed by the parameter $X_{\text{true}}^{\text{amp}}$. Because the distributions of e^{amp} and e^{ang} will be influenced by environmental factors, e.g., humidity, temperature, load level, and so on, the distributions may vary during long time periods [34]. Thus, in (7), a large n value is not recommended, and the value of n can be set to a number of sampling points during which the environmental factors have little influence on the distribution, e.g., the number of points in a time period of 0.5 s [35]. According to (7), the best estimated values $\hat{X}_{\text{true}}^{\text{amp}}$ and $\hat{X}_{\text{true}}^{\text{ang}}$ can be obtained. Then, substituting the estimated results obtained from (7) into (4), the estimations of parameters of the transmission line can be obtained as follows:

$$\begin{cases} \hat{z}_1 = \hat{r}_1 + i\hat{x}_1 = \hat{\gamma}\,\hat{z}_c \\ \hat{y}_1 = i\hat{b}_1 = \hat{\gamma}/\hat{z}_c \\ \hat{\gamma} = \dfrac{1}{D}\cosh^{-1}\left(\dfrac{\hat{U}_M^t \hat{I}_M^t \angle(\hat{\theta}_M^t + \hat{\phi}_M^t) - \hat{U}_N^t \hat{I}_N^t \angle(\hat{\theta}_N^t + \hat{\phi}_N^t)}{\hat{U}_N^t \hat{I}_M^t \angle(\hat{\theta}_N^t + \hat{\phi}_M^t) - \hat{U}_M^t \hat{I}_N^t \angle(\hat{\theta}_M^t + \hat{\phi}_N^t)}\right) \\ \hat{z}_c = \sqrt{\dfrac{(\hat{U}_M^t)^2 \angle(2\hat{\theta}_M^t) - (\hat{U}_N^t)^2 \angle(2\hat{\theta}_N^t)}{(\hat{I}_M^t)^2 \angle(2\hat{\phi}_M^t) - (\hat{I}_N^t)^2 \angle(2\hat{\phi}_N^t)}}. \end{cases} \tag{8}$$

By solving (8), the estimated values $\hat{z}_1$ and $\hat{y}_1$ can be obtained. In addition, these estimated values will largely reduce the uncertainty in the measurements. In Section IV, the parameters' evaluation will be illustrated specifically based on a practical transmission line model and the uncertainties in measurements subject to normal distributions.

After obtaining the estimated parameters of the transmission line, we can use following equation and measured phasors after a fault occurs to obtain the fault location L:

$$L = \frac{\dot{U}_{M1} - \dot{U}_{N1} + D(\hat{r}_1 + i\hat{x}_1)\dot{I}_{N1}'}{D(\hat{r}_1 + i\hat{x}_1)(\dot{I}_{M1}' + \dot{I}_{N1}')}. \tag{9}$$

The nomenclature, illustration, and derivation can be found in the Appendix.

TABLE II
TRANSMISSION LINE PARAMETERS

Sequence	Resistance (Ω/km)	Inductance (H/km)	Capacitance (F/km)
Positive	0.0386	$1.02846 \cdot 10^{-3}$	$11.575 \cdot 10^{-9}$
Zero	0.2955	$3.377 \cdot 10^{-3}$	$7.2 \cdot 10^{-9}$

TABLE III
PARAMETERS OF THE SOURCES

Terminal	Voltage (kV)	Angle (degree)	Impedance (Ω)
M	400	30	$0.1014 + i8.0133$
N	400	0	$1.128 + i16.0391$

TABLE IV
PARAMETERS OF THE UNCERTAINTY DISTRIBUTIONS

Distributions	Expectation	Standard Deviation
e_{MU}	0.0001	$5 \cdot 10^{-3}$
e_{NU}	0	$5 \cdot 10^{-3}$
e_{MI}	0.0003	$5 \cdot 10^{-3}$
e_{NI}	0	$5 \cdot 10^{-3}$
$e_{M\theta}$	0.001 rad	$5.8 \cdot 10^{-3}$
$e_{N\theta}$	0 rad	$5.8 \cdot 10^{-3}$
$e_{M\phi}$	0.001 rad	$8.7 \cdot 10^{-3}$
$e_{N\phi}$	0 rad	$8.7 \cdot 10^{-3}$

V. CASE STUDY

In Section V-A, a simulation case study will be presented to show the influence of the uncertainty in the measurements on the fault location algorithm and the effectiveness of the proposed uncertainty reduction method. In addition, the influence of the uncertainty in the measurements on the parameter evaluation and the positive sequence impedance fault location method will be analyzed. In Section V-B, the effectiveness of the proposed MLE method will be illustrated.

A. Background Setup

The transmission line used in this case study is a 500-km-long transmission line whose standard fundamental frequency is 50 Hz and its topology is shown in Fig. 1 [36]. The parameters of this transmission line are listed in Table II. The parameters of the sources at the *M* terminal and the *N* terminal are listed in Table III where the "Voltage" and "Current" represent the line-to-line voltage and current, respectively. The PMUs compute the current and voltage phasors 50 times per second. The number of samples n in (7) is 25 [35] where during a period of 0.5 s, environmental factors have little influence on the distributions of the uncertainties in the measurements. In addition, the distributions of the uncertainties in the measurements are assumed to be normal distributions whose parameters are listed in Table IV where the unit of the angle error is "rad."

This article has been accepted for inclusion in a future issue of this journal. Content is final as presented, with the exception of pagination.

FU *et al.*: INFLUENCE OF MEASUREMENT UNCERTAINTY ON PARAMETER ESTIMATION AND FAULT LOCATION FOR TRANSMISSION LINES 5

Phasor	Amplitude (kV or kA)	Angle (degree)
U_M^t	188.4414	28.02
U_N^t	186.7095	3.8564
I_M^t	0.8131	28.6925
I_N^t	0.7931	-165.7
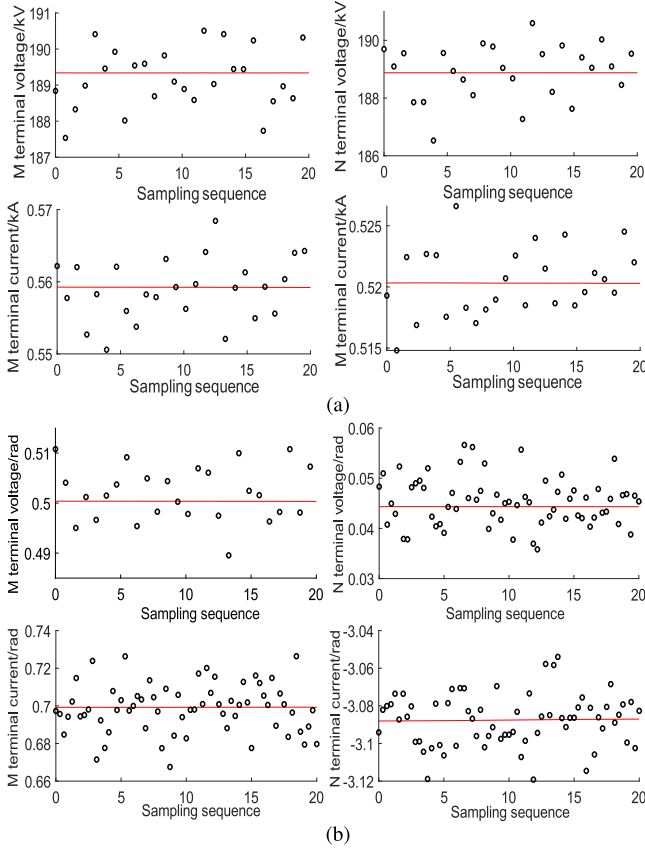
Fig. 2.   Distorted phasors. (a) Distorted phasor amplitudes. (b) Distorted phasor angles.

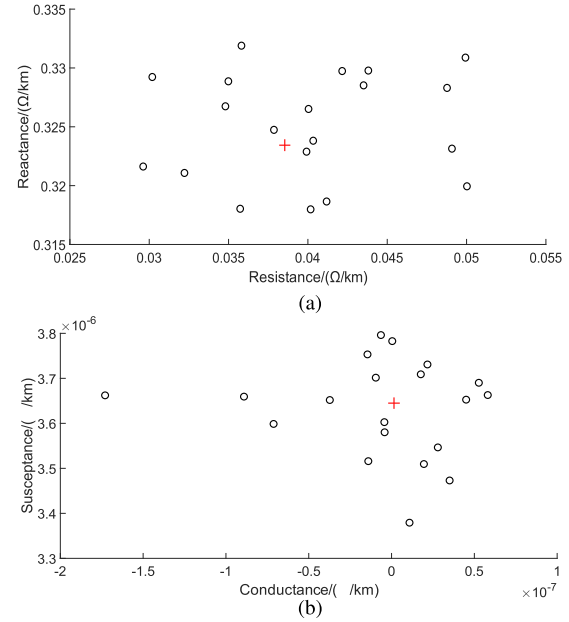Fig. 3.   Distorted positive sequence transmission line parameters. (a) Distorted positive sequence impedance. (b) Distorted positive sequence admittance.

B. Influence of Uncertainty in Measurements on Fault Location

During the normal operation status (no faults occurring), the true value of the voltage and current phasors at the *M* and *N* terminals simulated by MATLAB/Simulink are listed in Table V. After adding the uncertainties, which are subject to the normal distributions whose parameters are shown in Table IV, to the measurements of the phasors, the phasors are distorted as seen in Fig. 2.

In Fig. 2, the red line represents the exact value and the circles represent values distorted by the uncertainty in the measurements. In Fig. 2 (a) and (b), 20 scenarios of the uncertainty are generated by a Monte Carlo method based on the distributions whose parameters are shown in Table IV. In Fig. 2, it can be seen that both the amplitudes and the angles are distorted slightly, within quite small intervals that are no larger than 2% in the amplitudes and not larger than 0.04/rad

in the angles. After substituting the distorted values into (4), the transmission line parameters can be evaluated, as shown in Fig. 3.

In Fig. 3, the positive sequence transmission line parameters distorted by the uncertainty in the measurements are indicated by circles, and the exact positive sequence transmission line parameters are indicated by red plusses. All these points are computed using the voltage and current phasors obtained from Fig. 2. According to Fig. 3, it can be seen that the variations of the transmission line parameters are large (16% for the impedance and 8% for the admittance). From Figs. 2 and 3, it can be concluded that even slight distortions in the measurements caused by the uncertainty in the measurements can result in large distortions in calculated transmission line parameters. Then, according to (9), the gaps between the fault location calculated by exact transmission line parameters and calculated by the distorted transmission line parameters are listed in Table VI.

In the practical operation of a transmission line, the fault can occur anywhere along the line, while different fault locations may cause different fault characters. Thus, different fault locations are usually considered when evaluating and examining the performance of a fault location algorithm. These fault location cases are usually dispersed along the line. Thus, in Table VI, we have selected five fault locations and the distances between these five fault locations; the *M* terminals are set to 50, 125, 250, 375, and 450 km, respectively. In addition, by considering five different fault locations, we also intend to examine whether our proposed MLE method is effective for all fault locations and whether the fault location gaps between the exact value and the calculated value are influenced by the different fault locations. Note that the gaps listed in Table VI are all relative values, so not absolute values. Thus, a positive or negative value represents whether the distance between the

TABLE VI

FAULT LOCATION GAPS CONSIDERING THE UNCERTAINTY IN THE MEASUREMENTS

Scenario	Fault location (km)				
	50 km	125 km	250 km	375 km	450 km
1	0.1	0.221	-0.187	-0.053	-0.318
2	-0.06	-0.125	-0.051	0.088	-0.366
3	-0.168	-0.032	0.178	0.890	0.002
4	0.327	-0.160	-0.036	-0.033	-1.161
5	-0.166	-0.005	0.049	-0.644	0.500
6	-0.271	0.241	0.014	0.449	0.910
7	0.333	0.112	-0.243	-0.214	0.724
8	-0.225	-0.14	-0.198	-0.201	0.035
9	0.446	0.023	0.144	0.081	0.564
10	0.325	0.062	0.042	0.026	0.944
11	0.048	0.067	-0.044	-0.026	0.023
12	-0.01	0.131	-0.095	-0.017	-0.253
13	0.104	-0.045	0.167	-0.023	-0.120
14	0.306	-0.052	0.146	-0.265	0.796
15	0.034	0.115	-0.054	-0.831	0.025
16	0.197	0.069	-0.337	-0.102	0.265
17	-0.184	0.044	0.089	0.885	0.957
18	0.270	0.012	0.328	0.097	0.065
19	0.146	0.138	-0.228	0.318	-0.404
20	0.113	0.157	0.203	0.067	0.98

calculated fault location and the M terminal is larger than or less than the distance between the exact fault location and the M terminal.

In Table VI, it can be seen that the gaps are large, and, even sometimes, the gap is larger than 1 km, which cannot be ignored in the practical fault maintenance. A gap larger than 1 km will actually result in an additional 2-km search work by the maintenance personnel, which means a large additional cost. In addition, from the comparison between the columns of Table VI, it can also be observed that the variance of gaps for the fault at 125 km is smaller than at any other location. That is because, during the fault location calculation [see (9)], the variance of the gaps is transmitted from the uncertainty in the measurements to the fault location result. Thus, the variance of the gaps changes following the changes in the parameters in (9), including the measured voltage and current values after a fault has occurred. It can be seen that the variances of the gaps for different fault locations are different because different fault locations lead to different measured voltages and currents after a fault has occurred. Moreover, because the different values of fault resistances also result in different voltage and current values after a fault has occurred, it can be inferred that the fault resistance also influences the variance of the gap.

C. Simulation Results of the Proposed Method

As illustrated earlier, the influence of the uncertainty in the measurements on the positive sequence impedance fault

location method cannot be neglected. Thus, this section is designed to show the effectiveness of the proposed method in reducing the uncertainty in the measurements.

First, the pdfs of e^{amp} and e^{ang} are normal distributions that can be expressed by $\hat{X}^{amp}_{true}$ and $\hat{X}^{ang}_{true}$ that are required to be estimated. Then, according to the pdfs of e^{amp} and e^{ang} and (5), the distributions of $X^{amp}_{collect}$ and $X^{ang}_{collect}$ can be expressed using $\hat{X}^{amp}_{true}$ and $\hat{X}^{ang}_{true}$, such that $X^{amp}_{collect} \sim N\left(\hat{X}^{amp}_{true}(1+\mu_{e^{mag}}), (\hat{X}^{amp}_{true}\sigma_{e^{mag}})^2\right)$ and $X^{ang}_{collect} \sim N\left(\hat{X}^{ang}_{true}(1+\mu_{e^{ang}}), (\hat{X}^{ang}_{true}\sigma_{e^{ang}})^2\right)$, where the pdfs of $X^{amp}_{collect}$ and $X^{ang}_{collect}$ are, respectively, $f_{x^{mag}}$ and $f_{x^{ang}}$ as defined in (6). Then, based on the pdfs, the parameters can be evaluated by substituting the sampled data into (7). The results of parameter estimations using MLE are shown in Fig. 4.

More specifically, Fig. 4 shows 20 scenarios of the uncertainty in the measurements. The red plus represents transmission line parameters obtained from the exact voltage and current phasors, and the circles represent parameters obtained from 25 sampled points under the uncertainty in the measurements by using the MLE method to reduce the uncertainty. It can be observed that the distortions of the resistance, reactance, and susceptance are, respectively, 0.67%, 0.05%, and 0.015%. Note that the value of the conductance is very small so that the distortion of the conductance can be neglected. Comparing the results of Figs. 3 and 4, the uncertainty in the measurements can be largely reduced by using the MLE method in estimating the transmission line parameters. Furthermore, gaps between the fault location
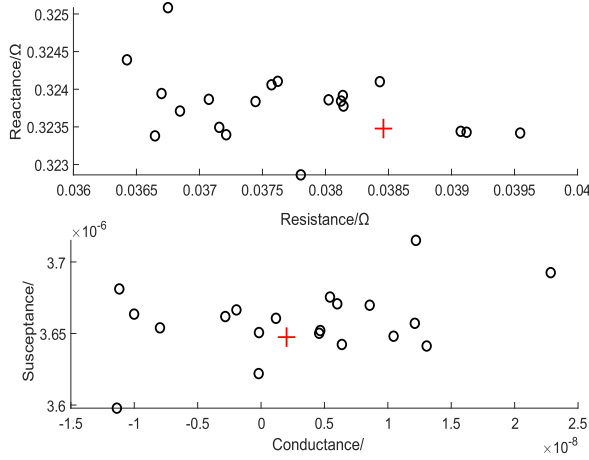
This article has been accepted for inclusion in a future issue of this journal. Content is final as presented, with the exception of pagination.

FU *et al.*: INFLUENCE OF MEASUREMENT UNCERTAINTY ON PARAMETER ESTIMATION AND FAULT LOCATION FOR TRANSMISSION LINES 7

Fig. 4.   Estimated transmission line parameters using MLE.

Fig. 5.   Positive sequence network of the transmission line.

results using exact transmission line parameters and the results using distorted parameters but addressed by the MLE method are shown in Table VII.

By comparing Table VI with Table VII, different from the analysis results of the Table VI, the gaps are no longer influenced by the measured terminal voltage and current phasors after a fault has occurred. It can also be observed that the gaps are largely reduced. Thus, the MLE method is suitable and effective to reduce the uncertainty in the measurements when the distributions of the measurement errors are known.

VI. CONCLUSION AND FUTURE WORK

This article has analyzed the influence of uncertainty in the measurements on the transmission line parameter estimations, which, in turn, influences the results of the fault location methods. In this analysis, we have used the classic two-terminal positive sequence network fault location algorithm as an example. We have adopted the MLE method to reduce the uncertainty in the measurements by using the distribution of the uncertainty. Simulation results show that even if the uncertainty in the measurements only causes a slight distortion in the measurements of less than 2%, the distortions on transmission line parameter calculations can be even larger than 10%. In addition, the gap between the calculated fault location and the exact fault location is sometimes larger than 1 km for a 500-km transmission line. Thus, the influence of the uncertainty in the measurements cannot be neglected. By using the proposed MLE method, both the distortion of the transmission line parameters and the gap between the calculated fault location and the exact fault location are at least ten times lower than when the proposed MLE method is not used. Thus, the proposed MLE method is suitable and effective to handle the uncertainty in the measurements.

Future work could investigate how to obtain more accurate stochastic distributions of phasor errors by using big data methods. The Bayesian inference might be an effective way to derive the error distributions by considering the different environmental factors that influence the errors in the measurements.
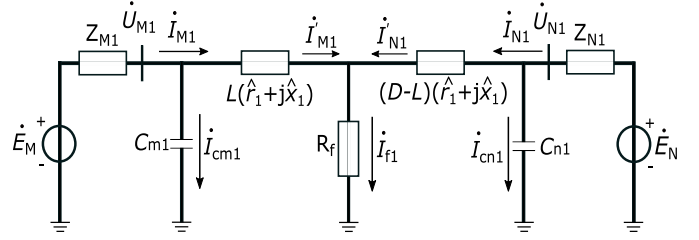
APPENDIX
FAULT LOCATION ALGORITHM

According to the mechanisms used in fault location algorithms, the fault location algorithms can be categorized into two main categories: fault analysis algorithms [37] and traveling-wave-based algorithms [38]. Both the fault analysis algorithms and traveling-wave-based algorithms are influenced by inaccurately measured transmission line parameters. In this article, we consider a typical fault analysis algorithm based on the two-terminal positive sequence impedance [39], which is widely applied for the transmission lines in China, because its performance is independent of source impedance variations, fault types, fault resistances, and fault distances. According to the pi model of the transmission line [40], the positive sequence network of the transmission line when a fault has occurred along the line can be explained using Fig. 5.

In Fig. 5, the fault occurs at the location that is L km away from the M terminal where the length of the whole transmission line is D km. Note that, in Fig. 5, all the impedance and conductance parameters are positive values. In detail, Z_{M1}, Z_{N1}, $C_{m1} = iD\hat{b}_1/2$, $C_{n1} = iD\hat{b}_1/2$, $L(\hat{r}_1 + i\hat{x}_1)$, $(D-L)(\hat{r}_1 + i\hat{x}_1)$, and R_f are, respectively, the M terminal equivalent impedance, N terminal equivalent impedance, shunt capacitance between the fault location and the M terminal, shunt capacitance between the fault location and the N terminal, impedance between fault location and the M terminal, impedance between fault location and the N terminal, and the fault resistance. In addition, $\hat{r}_1$, $\hat{x}_1$, and $\hat{b}_1$ are evaluated transmission line parameters that can be obtained by (8). Note that all the phasors in Fig. 5 are fault components of the positive sequence network by extracting the fault components from the positive symmetrical components [41]. In detail, $\dot{E}_M$, $\dot{U}_{M1}$, $\dot{I}_{M1}$, $\dot{I}_{cm1}$, and $\dot{I}'_{M1}$ are, respectively, the voltage of the M terminal source, voltage at M terminal, current at M terminal, current of shunt capacitance of the M terminal side, and current from the M terminal injecting into the fault point. The phasors for the N terminal are defined similarly. Furthermore, $\dot{I}_{f1}$ is the current flowing through the fault resistance. Then, Kirchhoff's law functions concerning the fault location can be formulated as follows:

$$\dot{U}_{M1} = L(\hat{r}_1 + i\hat{x}_1)\dot{I}_{M1} + \dot{U}_{f1} \tag{10a}$$

$$\dot{U}_{N1} = (D - L)(\hat{r}_1 + i\hat{x}_1)\dot{I}_{N1} + \dot{U}_{f1} \tag{10b}$$

$$\dot{I}_{cm1} = iD\hat{b}_1\dot{U}_{M1}/2 \tag{10c}$$

$$\dot{I}_{cn1} = iD\hat{b}_1\dot{U}_{N1}/2 \tag{10d}$$

$$\dot{I}'_{M1} = \dot{I}_{M1} - \dot{I}_{cm1} \tag{10e}$$

TABLE VII
FAULT LOCATION GAPS BY USING THE MLE METHOD

Scenario	Fault location (km)				
	50 km	125 km	250 km	375 km	450 km
1	-0.00375	0.011	0.0048	-0.0530	-0.0495
2	-0.0083	-0.0193	-0.0124	-0.0571	-0.0400
3	0.0179	0.0066	-0.0007	0.0213	0.0585
4	0.0385	-0.0036	-0.0125	-0.1095	0.0917
5	-0.0340	-0.0015	-0.0525	-0.0114	-0.0499
6	0.0438	0.0205	0.0143	0.0055	0.0720
7	0.0233	0.0054	-0.0014	0.0082	-0.0068
8	0.0212	0.0019	-0.0079	-0.0516	0.1116
9	0.0035	-0.0125	-0.0229	-0.0119	0.0200
10	0.0270	0.0118	0.0029	0.0012	0.0216
11	0.0125	-0.0267	-0.0062	0.0604	-0.0377
12	0.0515	0.0235	0.0140	0.0053	0.0770
13	0.0011	-0.0041	-0.0166	-0.0131	-0.0712
14	-0.0033	0.0151	-0.0194	0.0082	-0.0051
15	0.0268	0.0094	-0.0097	-0.0203	0.0458
16	0.0568	-0.0115	0.0013	-0.0274	0.0777
17	-0.0057	-0.0125	-0.0117	-0.0438	0.0423
18	0.0390	0.0118	0.0146	0.0130	-0.0269
19	0.0404	-0.0069	-0.0132	0.0371	-0.0005
20	0.0033	0.0073	-0.0172	0.0959	-0.0277

$$\dot{I}'_{N1} = \dot{I}_{N1} - \dot{I}_{cn1} \qquad (10f)$$

where ω is the angular velocity of the ac current. From (10), we can derive the final fault location

$$L = \frac{\dot{U}_{M1} - \dot{U}_{N1} + D(\hat{r}_1 + i\hat{x}_1)\dot{I}'_{N1}}{D(\hat{r}_1 + i\hat{x}_1)(\dot{I}'_{M1} + \dot{I}'_{N1})}. \qquad (11)$$

After substituting (10c)–(10f) into (11), the fault location L can be expressed using the measured phasors $\dot{U}_{M1}$, $\dot{I}_{M1}$, $\dot{U}_{N1}$, and $\dot{I}_{N1}$ that are collected after a fault has occurred. In practice, the expression of the fault location has fluctuations during an electromagnetic transient stage. Thus, a criterion should be used to derive the fault location result, such that if the gap between the L value at time step t_0 and that at the next time step $t_0 + 1$ is less than a threshold τ, then the fault location at time t_0 is L.

REFERENCES

[1] *IEEE Guide for Determining Fault Location on AC Transmission and Distribution Lines—Redline*, IEEE Standard C37.114-2014, Jan. 2015, pp. 1–128.

[2] Y. Q. Chen, O. Fink, and G. Sansavini, "Combined fault location and classification for power transmission lines fault diagnosis with integrated feature extraction," *IEEE Trans. Ind. Electron.*, vol. 65, no. 1, pp. 561–569, Jan. 2018.

[3] D. Carrión, J. W. González, I. A. Issac, and G. J. Lopez, "Optimal fault location in transmission lines using hybrid method," in *Proc. IEEE PES Innov. Smart Grid Technol. Conf.-Latin Amer. (ISGT Latin America)*, Sep. 2017, pp. 1–6.

[4] G. Song, J. Suonan, Q. Xu, P. Chen, and Y. Ge, "Parallel transmission lines fault location algorithm based on differential component net," *IEEE Trans. Power Del.*, vol. 20, no. 4, pp. 2396–2406, Oct. 2005.

[5] V. Terzija, G. Preston, V. Stanojević, N. I. Elkalashy, and M. Popov, "Synchronized measurements-based algorithm for short transmission line fault analysis," *IEEE Trans. Smart Grid*, vol. 6, no. 6, pp. 2639–2648, Nov. 2015.

[6] A. S. Dobakhshari, "Fast accurate fault location on transmission system utilizing wide-area unsynchronized measurements," *Int. J. Electr. Power Energy Syst.*, vol. 101, pp. 234–242, Oct. 2018.

[7] S. A. Soliman, R. A. Alammari, and M. E. El-Hawary, "A new digital transformation for harmonics and DC offset removal for the distance fault locator algorithm," *Int. J. Electr. Power Energy Syst.*, vol. 26, no. 5, pp. 389–395, Jun. 2004.

[8] M. Tajdinian, M. Z. Jahromi, K. Mohseni, and S. M. Kouhsari, "An analytical approach for removal of decaying DC component considering frequency deviation," *Electr. Power Syst. Res.*, vol. 130, pp. 208–219, Jan. 2016.

[9] J. F. M. Argüelles, M. A. Z. Arrieta, J. L. Domínguez, B. L. Jaurrieta, and M. S. Benito, "A new method for decaying DC offset removal for digital protective relays," *Electr. Power Syst. Res.*, vol. 76, no. 4, pp. 194–199, Jan. 2006.

[10] J. Lázaro, J. F. Miñambres, and M. A. Zorrozua, "Selective estimation of harmonic components in noisy electrical signals for protective relaying purposes," *Int. J. Electr. Power Energy Syst.*, vol. 56, pp. 140–146, Mar. 2014.

[11] K. K. Sharma, "New algorithms for removal of DC offset and subsynchronous resonance terms in the current and voltage signals under fault conditions," *WSEAS Trans. Power Syst.*, vol. 9, pp. 103–110, Jan. 2014.

[12] I. M. Karmacharya and R. Gokaraju, "Fault location in ungrounded photovoltaic system using wavelets and ANN," *IEEE Trans. Power Del.*, vol. 33, no. 2, pp. 549–559, Apr. 2018.

[13] P. K. Dash, S. R. Samantaray, G. Panda, and B. K. Panigrahi, "Time–frequency transform approach for protection of parallel transmission lines," *IET Gener., Transmiss. Distrib.*, vol. 1, no. 1, pp. 30–38, 2007.

[14] K. R. Krishnanand, P. K. Dash, and M. H. Naeem, "Detection, classification, and location of faults in power transmission lines," *Int. J. Electr. Power Energy Syst.*, vol. 67, pp. 76–86, May 2015.

[15] M. Picallo, A. Anta, and B. de Schutter, "Comparison of bounds for optimal PMU placement for state estimation in distribution grids," *IEEE Trans. Power Syst.*, vol. 34, no. 6, pp. 4837–4846, Nov. 2019.

This article has been accepted for inclusion in a future issue of this journal. Content is final as presented, with the exception of pagination.

FU *et al.*: INFLUENCE OF MEASUREMENT UNCERTAINTY ON PARAMETER ESTIMATION AND FAULT LOCATION FOR TRANSMISSION LINES 9

[16] T. Bi, H. Liu, D. Zhang, and Q. Yang, "The PMU dynamic performance evaluation and the comparison of PMU standards," in *Proc. IEEE Power Energy Soc. Gen. Meeting*, Jul. 2012, pp. 1–5.

[17] Q. Jiang, X. Li, B. Wang, and H. Wang, "PMU-based fault location using voltage measurements in large transmission networks," *IEEE Trans. Power Del.*, vol. 27, no. 3, pp. 1644–1652, Jul. 2012.

[18] D. Ritzmann, P. S. Wright, W. Holderbaum, and B. Potter, "A method for accurate transmission line impedance parameter estimation," *IEEE Trans. Instrum. Meas.*, vol. 65, no. 10, pp. 2204–2213, Oct. 2016.

[19] G. Sivanagaraju, S. Chakrabarti, and S. C. Srivastava, "Uncertainty in transmission line parameters: Estimation and impact on line current differential protection," *IEEE Trans. Instrum. Meas.*, vol. 63, no. 6, pp. 1496–1504, Jun. 2014.

[20] M. Asprou, E. Kyriakides, and M. M. Albu, "Uncertainty bounds of transmission line parameters estimated from synchronized measurements," *IEEE Trans. Instrum. Meas.*, vol. 68, no. 8, pp. 2808–2818, Aug. 2019.

[21] V. Milojević, S. Čalija, G. Rietveld, M. V. Acanski, and D. Colangelo, "Utilization of PMU measurements for three-phase line parameter estimation in power systems," *IEEE Trans. Instrum. Meas.*, vol. 67, no. 10, pp. 2453–2462, Oct. 2018.

[22] N. M. Manousakis, G. N. Korres, and P. S. Georgilakis, "Taxonomy of PMU placement methodologies," *IEEE Trans. Power Syst.*, vol. 27, no. 2, pp. 1070–1077, May 2012.

[23] J. Suonan, S. Gao, G. Song, Z. Jiao, and X. Kang, "A novel fault-location method for HVDC transmission lines," *IEEE Trans. Power Del.*, vol. 25, no. 2, pp. 1203–1209, Apr. 2010.

[24] L. Yuansheng, W. Gang, and L. Haifeng, "Time-domain fault-location method on HVDC transmission lines under unsynchronized two-end measurement and uncertain line parameters," *IEEE Trans. Power Del.*, vol. 30, no. 3, pp. 1031–1038, Jun. 2015.

[25] J.-A. Jiang, J.-Z. Yang, Y.-H. Lin, C.-W. Liu, and J.-C. Ma, "An adaptive PMU based fault detection/location technique for transmission lines. I. Theory and algorithms," *IEEE Trans. Power Del.*, vol. 15, no. 2, pp. 486–493, Apr. 2000.

[26] L. Tang, X. Dong, S. Luo, S. Shi, and B. Wang, "A new differential protection of transmission line based on equivalent travelling wave," *IEEE Trans. Power Del.*, vol. 32, no. 3, pp. 1359–1369, Jun. 2017.

[27] C. Wang, Q.-Q. Jia, X.-B. Li, and C.-X. Dou, "Fault location using synchronized sequence measurements," *Int. J. Electr. Power Energy Syst.*, vol. 30, no. 2, pp. 134–139, Feb. 2008.

[28] D. F. Howard, T. G. Habetler, and R. G. Harley, "Improved sequence network model of wind turbine generators for short-circuit studies," *IEEE Trans. Energy Convers.*, vol. 27, no. 4, pp. 968–977, Dec. 2012.

[29] Y. Zhong, X. Kang, Z. Jiao, Z. Wang, and J. Suonan, "A novel distance protection algorithm for the phase-ground fault," *IEEE Trans. Power Del.*, vol. 29, no. 4, pp. 1718–1725, Aug. 2014.

[30] *Evaluation of Measurement Data—Guide to the Expression of Uncertainty in Measurement*, document JCGM 100:2008, International Organization for Standardization, 2008, vol. 50, p. 134.

[31] M. Šíra, S. Mašlán, V. N. Zachovalová, G. Crotti, and D. Giordano, "Modelling of PMU uncertainty by means of Monte Carlo method," in *Proc. Conf. Precis. Electromagn. Meas. (CPEM)*, Jul. 2016, pp. 1–2.

[32] Arbiter Systems, Paso Robles, CA, USA. (2006). *Model 1133 GPS-Synchronized Power Quality/Revenue Standard Operation Manual*. [Online]. Available: https://www.arbiter.com/files/product-attachments/1133a_manual.pdf

[33] S. Chakrabarti, E. Kyriakides, and M. Albu, "Uncertainty in power system state variables obtained through synchronized measurements," *IEEE Trans. Instrum. Meas.*, vol. 58, no. 8, pp. 2452–2458, Aug. 2009.

[34] C. Li, Y. Zhang, H. Zhang, Q. Wu, and V. Terzija, "Measurement-based transmission line parameter estimation with adaptive data selection scheme," *IEEE Trans. Smart Grid*, vol. 9, no. 6, pp. 5764–5773, Nov. 2018.

[35] K. V. Khandeparkar, S. A. Soman, and G. Gajjar, "Detection and correction of systematic errors in instrument transformers along with line parameter estimation using PMU data," *IEEE Trans. Power Syst.*, vol. 32, no. 4, pp. 3089–3098, Jul. 2017.

[36] J. Xia, X. Zhang, X. Huang, X. Kang, W. Shao, and Y. Liu, "Fault locating based on longitudinal impedance according to dual terminal variables," *Electr. Power Autom. Equip.*, vol. 35, no. 10, pp. 133–139, 2015.

[37] J. Mora-Florez, J. Meléndez, and G. Carrillo-Caicedo, "Comparison of impedance based fault location methods for power distribution systems," *Electr. Power Syst. Res.*, vol. 78, no. 4, pp. 657–666, Apr. 2008.

[38] P. Crossley, M. Davidson, and P. Gale, "Fault location using travelling waves," in *Proc. IEEE Colloq. Instrum. Electr. Supply Ind.*, Jun. 1993, pp. 1–6.

[39] J. Xianing, W. Fuping, and W. Zanji, "Research on fault location based on dynamic synchronous phasor measurement by PMU," *Power Syst. Technol.*, vol. 37, no. 10, pp. 2932–2937, 2013.

[40] M. S. Sachdev and R. Agarwal, "A technique for estimating transmission line fault locations from digital impedance relay measurements," *IEEE Trans. Power Del.*, vol. 3, no. 1, pp. 121–129, Jan. 1988.

[41] H. Gao and P. A. Crossley, "Design and evaluation of a directional algorithm for transmission-line protection based on positive-sequence fault components," *IEE Proc.-Gener., Transmiss. Distrib.*, vol. 153, no. 6, pp. 711–718, 2006.

Jianfeng Fu received the master's degree from Xi'an Jiaotong University, Xi'an, China. He is currently pursuing the Ph.D. degree with the Delft University of Technology, Delft, The Netherlands.

He is working on power system maintenance and operation research.

Guobing Song (Member, IEEE) was born in Henan, China, in February 1972. He received the Ph.D. degree in electrical engineering from Xi'an Jiaotong University, Xi'an, China, in 2005.

He is currently a Full Professor with the School of Electrical Engineering, Xi'an Jiaotong University. His research interests include transmission line fault location and protection.

Bart De Schutter (Fellow, IEEE) is currently a Full Professor and the Head of the Department with the Delft Center for Systems and Control, Delft University of Technology, Delft, The Netherlands. His current research interests include intelligent transportation, infrastructure, power systems, hybrid systems, and multilevel control.

Dr. De Schutter is a Senior Editor of the IEEE TRANSACTIONS ON INTELLIGENT TRANSPORTATION SYSTEMS.